https://doi.org/10.14669/AM.VOL95.ART2

MEASUREMENT OF THE FRICTION PARAMETERS OF A BELT TRANSMISSION UNDER HEAVY LOAD

KRZYSZTOF KUBAS[1]

Abstract

This article presents the results of measurements of a belt transmission with a poly-V belt 5PK, most often used in the industry, especially in industrial drives, agricultural machines and in the automotive industry. The main goal of the works was to obtain the dependence of the belt slip value on the measured, relatively high values of resistance torque. For this purpose, a series of measurements were made using a specialised research stand consisting of two alternating current motors and attached pulleys. It considered four cases of the value of the belt pre-tensioning force. In each of the cases, while making the measurements, the resistance of the passive pulley was increased, resulting in increasing values of belt slip. Finally, the achieved courses were approximated. The obtained results will be used to develop empirical models of friction at the belt-pulley interface. They can also be useful for belt manufacturers to make better belts, especially those subjected to higher loads.

Keywords: poly-V belt; belt transmission; belt slip; measurements; belt-pulley friction

1. Introduction

Exemplary works presenting the measurements of a poly-V belt are [1, 2], [6–8], and also [17, 26] where, among other parameters, frictional parameters have been measured. In the works, the results of measurements of belt slip, as well as contact forces between the poly-V belt and the pulley, can be found, along with longitudinal and bending stiffness and damping. Some of these works include measurements of contaminated belt. Particularly noteworthy are publications [1, 26], due to the similar subject matter of the works.

Among the works covering the research, one can also cite paper [14], in which the elastic properties of a multi-V belt together with the load-bearing layer were measured. The tests included stretching the belt and compressing the rubber. It also worth mentioning articles [10, 13, 23], also [27, 32] in which the friction of contaminated rubber and wear processes were investigated. It is also worth mentioning works [24, 25, 31], which investigate power losses in belt transmissions and the influence of material types and initial belt tension on the friction coefficient.

1 Department of Combustion Engines and Vehicles, University of Bielsko-Biała, Willowa 2, 43-309 Bielsko-Biała, Poland, e-mail: kkubas@ath.bielsko.pl, ORCID: 0000-0002-3594-8665

https://doi.org/10.14669/AM.VOL95.ART2

Measurements of belt transmissions are can be useful to develop more and more friction models of belt transmissions. The development of these models, which accurately reflect the behaviour of the friction belt along the pulley, was dealt with by, among others, Leamy et al. [20, 22] developing so-called "Piecewise linear friction models", including the "Coulomb-like tri-linear creep-rate-dependent friction law", as well as Kim [16] developing the "elastic / perfectly plastic friction law". One can also find works using commonly used friction models, such as the Brush model [5, 12], the Dahl model [18], or the GMS model [19].

It is also worth mentioning that generally there are two groups of models of the belt: discrete and non-discrete models. Studies of discrete belt models have been presented in [15, 21, 22]. Non-discrete belt models can be modelled as an elastic rod (papers [3, 4, 29]), a string with assumed longitudinal and bending stiffness (papers [9, 11, 28] and [30]). Of course, regardless of the adopted belt models and models of friction at the belt-pulley contact, there is always a need to adjust the number of coefficients adopted in them, which will ensure the compatibility of these models with the real object. Thus, there is a constant need to obtain the results of experimental tests of a transmission performed in various operating conditions. The results presented in this article should therefore be taken as complementary to the work of previous authors dealing with similar topics.

2. The measured transmission

Figure 1 shows the analysed belt transmission. Additionally, Figure 2 presents schematically measured transmission input and output parameters. The transmission consists of two pulleys (1) and (2) with a 5PK 1200 belt (3). These types of belts are found primarily in the automotive industry, especially in alternators and air-conditioning compressor drive systems. In such cases, the driving wheel is driven by the vehicle's engine.

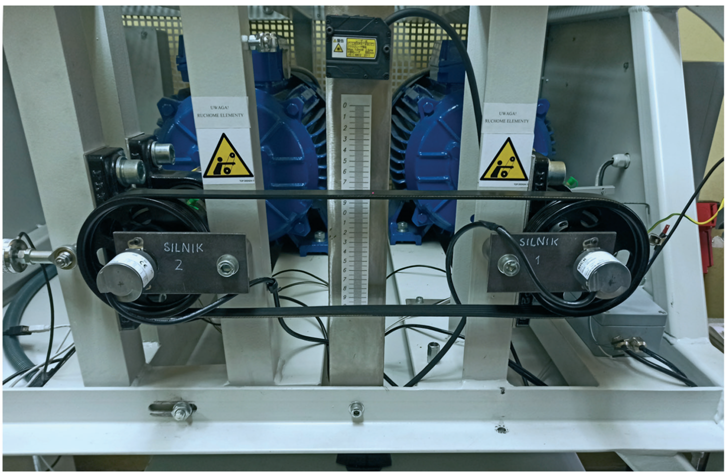

Fig. 1. Research stand with the measured belt transmission

https://doi.org/10.14669/AM.VOL95.ART2

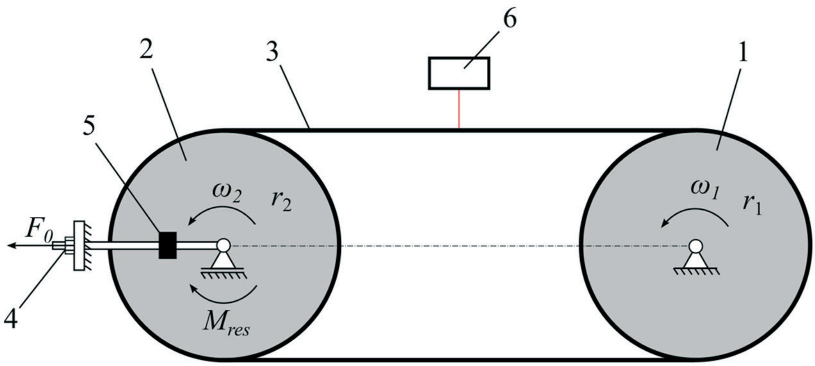

Fig. 2. Scheme of the measured system with a belt transmission

To simplify the measurements, it was assumed that the pulleys have the same radius of r_1=r_2=0.06 m. The transmission can be tensioned by a screw and a bolt (4) moving the left pulley. The tensioning force F_0 can be measured by a force sensor (5) connected to the screw. It applied rotational velocities ω_1 and ω_2 by manually changing the velocities of two electric motors. The velocities are measured by incremental sensors connected to the shafts. If both velocities are equal, the transmission rotates without any load. A test stand designed in such a way allows the simulation of situations which slips occurring. Reducing the velocity of the second pulley causes resistance torque M_{res}.

Various rotational velocities of the motors were realised by means of inverters. Therefore, one should be aware of the difficulties of such a solution. There is a high probability that slip will occur in the magnetic fields of the rotors (especially in cases of large resistance torque M_{res}). However, this difficulty does not affect the reliability of the results, because both rotational speeds and the moment of resistance are measured simultaneously.

Additionally, such a system allows for the measurement of vibrations of the slack part of the belt via a laser sensor (6) placed in the middle between the two pulleys. Vibrations of the slack part of the belt result only from its compliance. Compliance in bearings, flexibility of the frame and longitudinal deformation of the screw can be ignored.

The transmission slip can be described as the following formula:

$$\omega_s = \omega_1 - \omega_2. \tag{1}$$

In certain situations, it may be more convenient to present its relative value as:

$$s = \frac{\omega_1 - \omega_2}{\omega_1} \cdot 100\% = \frac{\omega_s}{\omega_1} \cdot 100\%. \tag{2}$$

https://doi.org/10.14669/AM.VOL95.ART2

In a situation in which the slip ω_s has positive values, the first motor spins at a higher speed value than the second ($\omega_1 > \omega_2$). The differences of angular velocities mainly result from existing nonzero values of resistance torque M_{res}. When the transmission has to be rapidly stopped, it is possible that inertia of the second pulley (with all masses connected to it) causes that $\omega_2 > \omega_1$. In this case, the values ω_s and s will be negative.

It is worth noting here that the values of the dynamic friction coefficient are often expressed as a function of the slip velocity in the friction connection, because the value of this coefficient does not have to be constant. In such a case, the values of the friction forces should be determined taking into account the slip ω_s. One of two types of characteristics can then be determined: kinetic characteristics of the friction coefficient (determined for the set sliding velocities) and dynamic characteristics of the friction coefficient (determined under the conditions of variable sliding velocities).

3. Results of measurements

It assumed that before each measurement, the angular velocities of the pulleys would be nearly the same and achieve a value of about 750 rpm. Next, decreased the velocity of the second motor to load the transmission. The measurements started just after noticing the nonzero resistance torque $Mres$. It was decided to achieve a value of about 30 Nm. As a result of the resistance torque, the first pulley was also loaded, which also resulted in a reduction in rotational speed ω_1.

It was also decided to consider four cases of belt tensioning force F_0 of: 500 N, 250 N, 125 N and 75 N. The first value is closest to the standard tensioning value. The assumed tensioning forces values of 250 N, 125 N were assumed as a half and a quarter of the standard value of the belt tension force in the transmission, respectively. The value of 75 N in the last case was assumed after the initial measurements of the working transmission and the possible measuring range of the belt displacement sensor. Moreover, it was decided that in the first two cases F_0=550 N and 250 N, the measurement would be completed as soon as the intended value of the moment of resistance M_{res}=30 Nm was reached. In the other two cases, it was decided that the measurement would be slightly extended to check how the slip values would change after reaching this value.

https://doi.org/10.14669/AM.VOL95.ART2

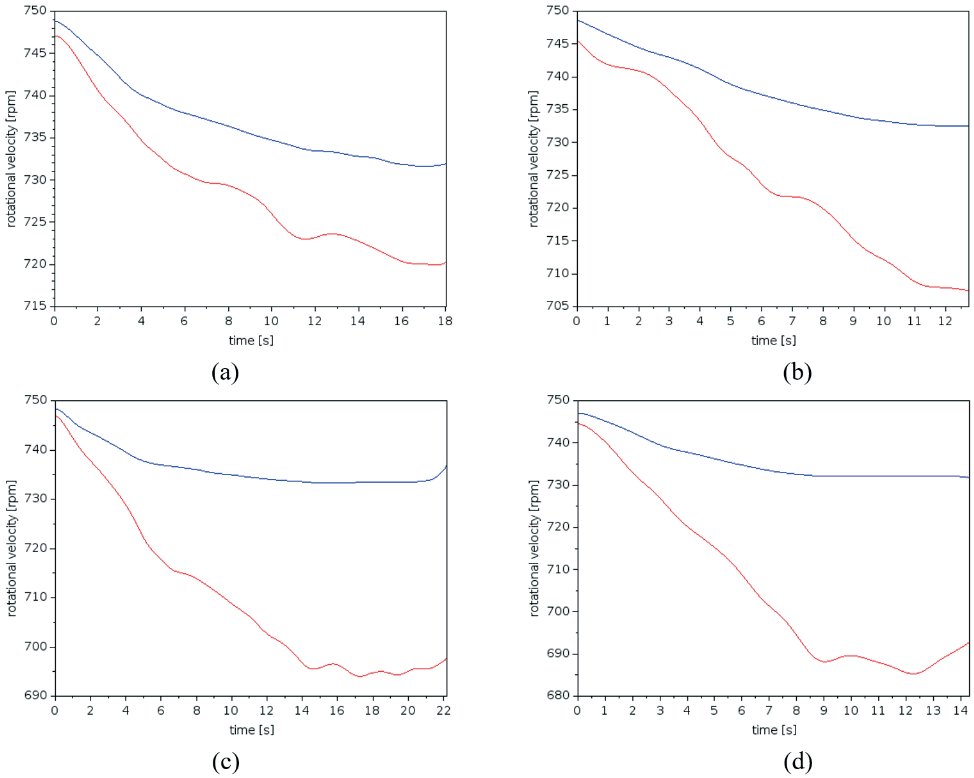

Fig. 3. Measured courses of rotational velocities of pulleys ω_1 (——) and ω_2 (——): (a) F_0=500 N, (b) F_0=250 N, (c) F_0=125 N, (d) F_0=75 N

Figure 3 shows the courses of the measured rotational velocities of pulleys, whereas Figure 4 presents the course of the measured resistance torque M_{res}. As can be noticed from both figures, with increasing discrepancy between rotational velocities, the resistance torque increased. However, the forms of the rotational speed courses of the pulleys ω_1 (upper courses) and ω_2 (lower courses), and the resulting course of the resistance torque M_{res}, are not similar. This is due to, among other factors, the fact that different frictional conditions occur around the circumference of the belt as well as changes in pressure forces during the operation of the transmission. Moreover, in cases of lower belt tensioning force F_0=125 N and 75 N (Figure 3c and Figure 3d), a slight increase in rotational speed ω_2 after reaching the intended value of the resistance torque M_{res} can be noticed. This is due to the extended measurement time assumed in both cases. Significant slip resulted in a change in the friction value due to the increase in belt temperature.

https://doi.org/10.14669/AM.VOL95.ART2

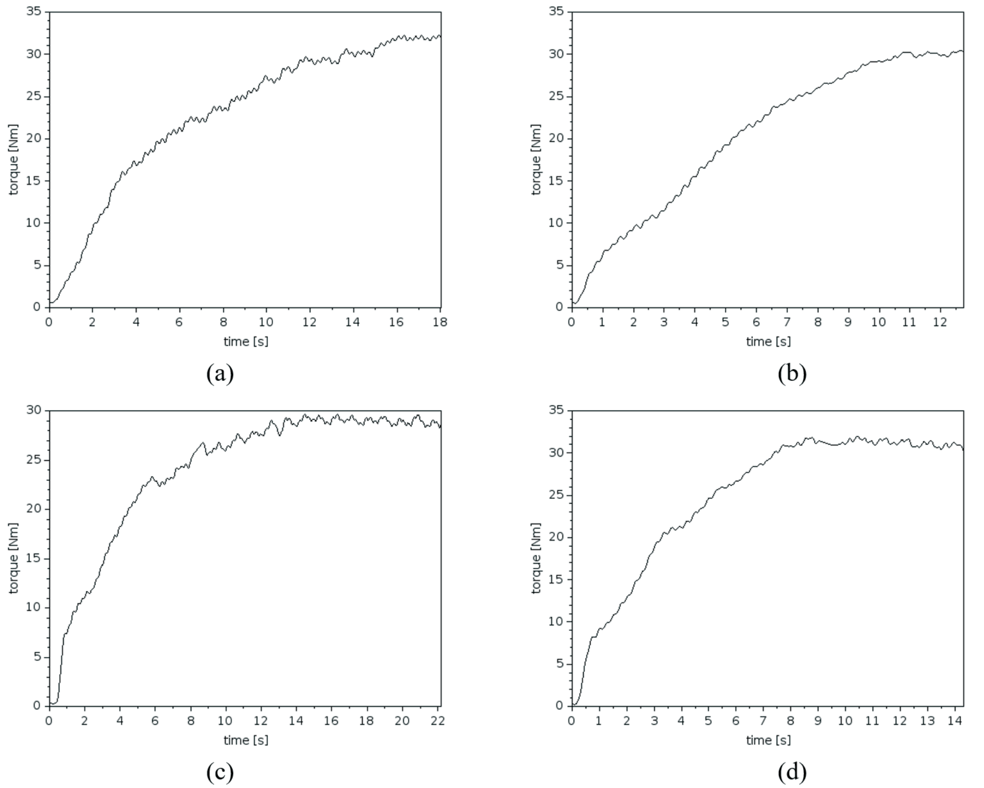

Fig. 4. Measured courses of resistance torque M_{res} in transmission:
(a) F_0=500 N, (b) F_0=250 N, (c) F_0=125 N, (d) F_0=75 N

In Figure 5, changes in the tensioning force during measurements are presented. As can be noticed, during the increase of resistance torque M_{res}, the tensioning force also increased, reaching even 800 N (in the case of F_0=75 N). Particularly interesting is that despite the assumed different initial values of tensioning force F_0, after achieving the assumed full resistance torque value, the tensioning force mostly achieves over 400 N. For the measured cases of F_0=250 N, 125 N and 75 N, the average values of tensioning force oscillate between 575 N (Figure 5b) to 520 N (Figure 5c). The first case (Figure 5a) seems to be an exception. There is a noticeable increase in the average value up to 660 N.

Figure 6 shows the waveforms of the measured belt slip values ω_s. As expected, as the values of the initial belt tension decrease, the values of the belt slip increase. Its highest value occurred at the moment of the highest moment of resistance. As can be seen from the figures shown, the slip was as follows: in case of F_0=500 N (Figure 6a) about $\omega_s=12$ rpm, which was about s=1.7%, in the case of F_0=250 N – ω_s=25 rpm (s=3.6%), F_0=125 N – ω_s=40 rpm (s=5.5%) and F_0=75 N – ω_s=47 rpm (s=6.4%). The obtained maximum slip values were compared with each other in the form of the points in Figure 7.

https://doi.org/10.14669/AM.VOL95.ART2

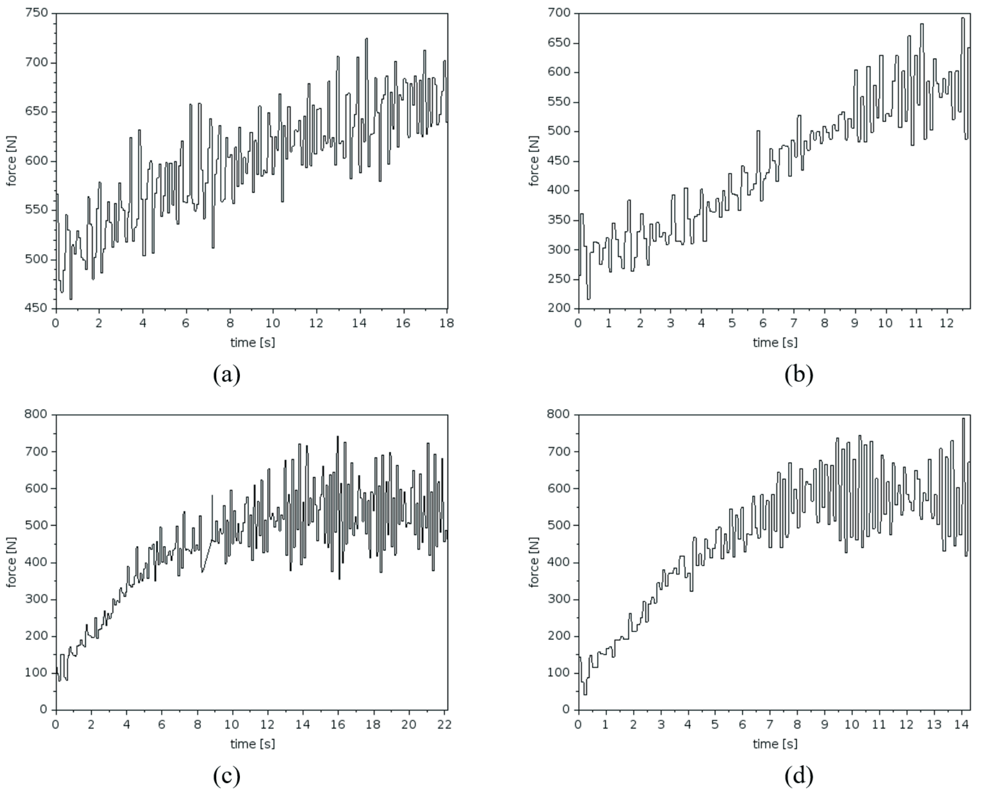

Fig. 5. Measured courses of tensioning force in transmission:
(a) F_0=500 N, (b) F_0=250 N, (c) F_0=125 N, (d) F_0=75 N

https://doi.org/10.14669/AM.VOL95.ART2

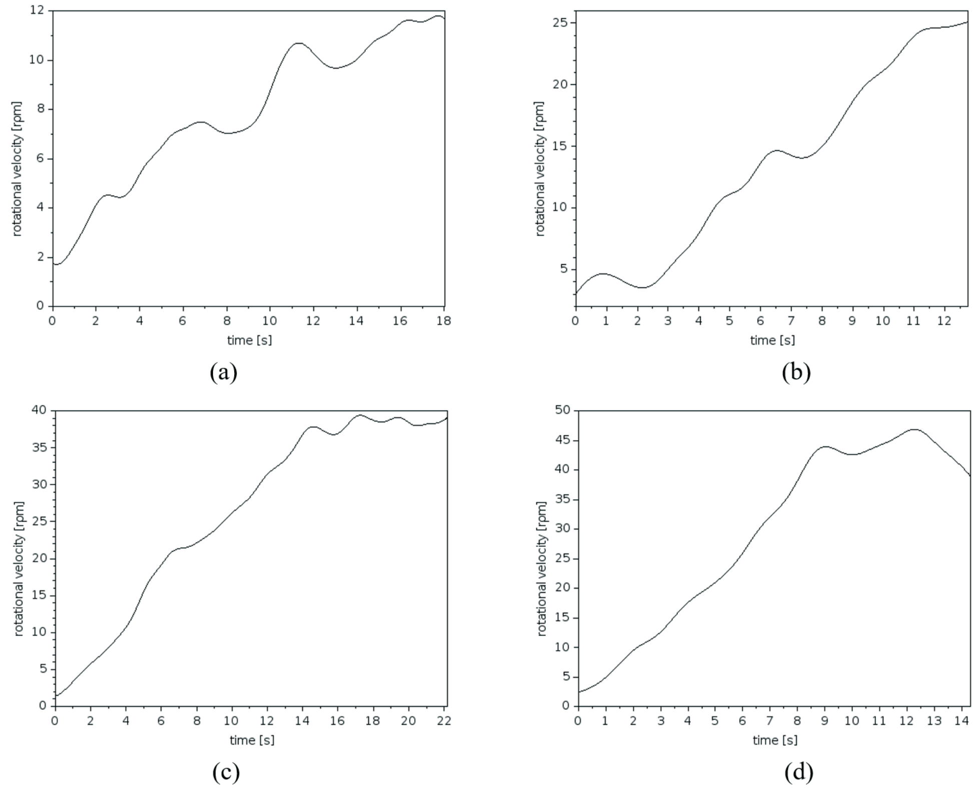

Fig. 6. Measured courses of belt slip as a rotational velocity: (a) F_0=500 N, (b) F_0=250 N, (c) F_0=125 N, (d) F_0=75 N

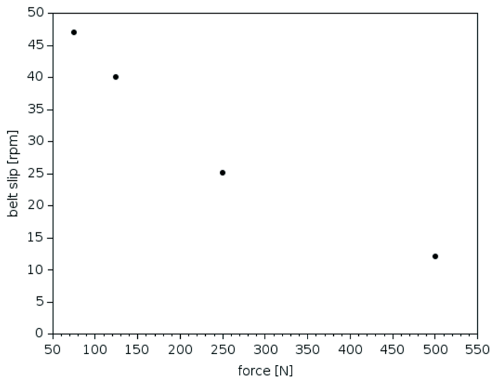

Fig. 7. Values of maximum measured values of belt slip ω_s in assumed cases of preload force F_0

https://doi.org/10.14669/AM.VOL95.ART2

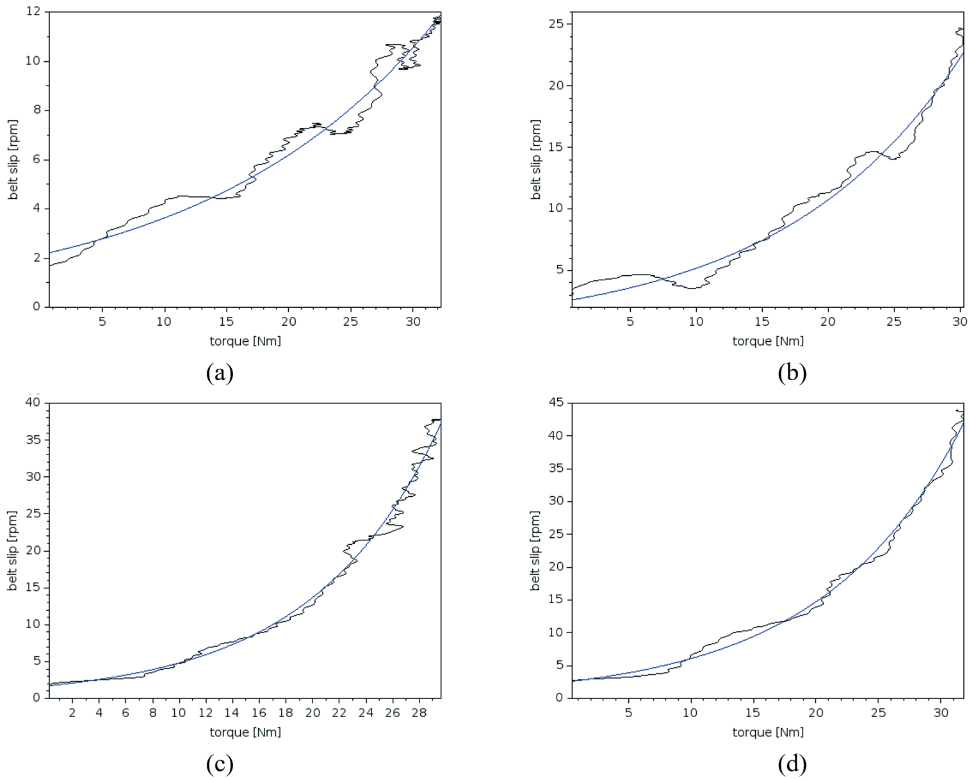

Fig. 8. Measured belt slip ω_s (——) and calculated approximation lines ω'_s (——) as a function of resistance torque: (a) F_0=500 N, (b) F_0=250 N, (c) F_0=125 N, (d) F_0=75 N

It is reasonable to present the value of the slip as a function of the resistance torque $\omega_s(M_{res})$ (Figure 8). As can be seen, this relationship seems to be linear in a certain time period only for F_0=500 N. Comparing the measured, presented dependence $\omega_s(M_{res})$ in Figure 8b–8d with the first in Figure 8a, the linear shape seems to disappear. For this reason, it was decided to approximate the selected fragment of the course (when torque M_{res} increases) with an exponential approximation. For this purpose, the following formula was obtained:

$$\omega'_s(M_{res}) = c_1 \cdot e^{c_2 \cdot M_{res}}, \qquad (3)$$

where:
c_1, c_2 – approximation coefficients.

In the approximation process, the searched coefficients c_1 and c_2 were determined. The change in the value of the c_1 coefficient caused the approximation curve to "move" vertically, while the change in the c_2 coefficient caused an increase in the slope of the curve, especially on its right side. It was chosen to minimise the norm given by the following formula:

https://doi.org/10.14669/AM.VOL95.ART2

$$N = \sqrt{\sum_{i=1}^{n_p} \left(\omega_s^i - {\omega'}_s^i\right)^2}, \tag{4}$$

where:
n_p – number of considered measurement points.

In Table 1, the calculated coefficients from the approximation process are presented. As can be seen from the presented results, regardless of the assumed value of the belt pre-tensioning force F_0, the values of the coefficient c_2 are similar to each other. The value of this coefficient seems to increase slightly with successive cases of decreasing force F_0. The discrepancy of the c_1 coefficient is much greater.

Table 1. Calculated coefficient of approximation curves

F_0 [N]	Selected time [s]	c_1	c_2	N
500	0–18	2.13541	0.0532388	21.2
250	0–12	2.49763	0.0729562	38.7
125	0–15	1.70297	0.1041835	56.5
75	0–9	2.50681	0.0885798	35.5

Figure 8 shows both the approximated fragment of the waveform (in the considered time period) and the obtained approximation line. The results are consistent to the results obtained by the authors of works [1, 26], with the difference being that in the quoted work, much lower values of resistance torque M_{res} were used (the values did not exceed 7 Nm). The results obtained in this study can therefore be treated as supplementary in a sense.

https://doi.org/10.14669/AM.VOL95.ART2

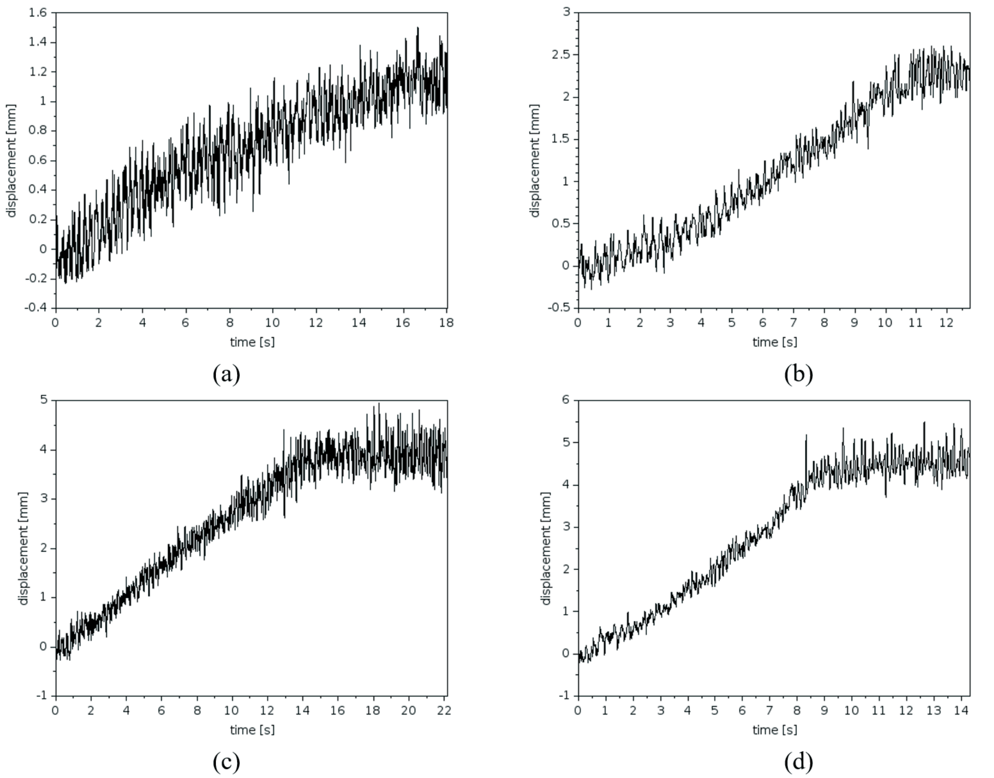

Fig. 9. Measured courses of displacement of slick part of the belt:
(a) F_0=500 N, (b) F_0=250 N, (c) F_0=125 N, (d) F_0=75 N

Figure 9 presents the measured displacement of the loose (upper) part of the belt. As can be seen from the figures, the loose part of the belt began to buckle simultaneously with increasing transmission velocity. However, the centrifugal forces were so large that they did not allow the belt to oscillate. In the case of F_0=500 N (Figure 9a), displacement has reached the value of 1.5 mm, but the instantaneous amplitude not exceed 0.7 mm. In the case of F_0=250 N (Figure 9b), the measured values of belt displacement of the deformed shape of the belt was about 2.6 mm; in the case of F_0=125 N (Figure 9c), it increased to about 5 mm; and in the case of F_0=75 N (Figure 9d), it changed to about 5.5 mm. It should be noted that the maximum values of the belt deflection depend on the transmission velocity causing centrifugal forces and the assumed values of the belt tensioning force F_0. It should also be noted that, as the speed increases, the belt reduces the wrap angle on the wheels, so the simultaneous increase in slip is also caused by this fact.

4. Conclusions

As mentioned in the introduction, the main goal of the discussed measurements was to investigate how the belt slip would increase under high loads. Earlier works, e.g. [1, 26], describe measurements results with much smaller values of resistance torque. Additionally, it was noticed that the slip values increase non-linearly during the increase of the resistance torque M_{res}.

It should be emphasized here that such high values of resistance torque, although rarely occurring in the actual operating conditions of the transmission, are not impossible. Such a situation may occur, for example, in the case of heavily worn parts of the alternator or air-conditioning system in the car, e.g. in situations of seized bearings in the alternator, when the rotor rubs against the stator.

It has been proven in the work that a load reaching even a value of M_{res}=30 Nm can also occur in the case of a less tensioned transmission. It is surprising that in such situations, the slip values did not exceed the value of 7%. Due to sufficient wedging of the belt in the grooves, part of the power can still be transferred to the driven pulley, although, of course, belt vibrations disqualify the transmission from further operation. It should be emphasised here that during the tests, efforts were made to not overheat the belt so that too much of a temperature change would not affect its frictional properties.

The obtained results will be used to develop empirical models of friction at the belt-pulley interface. It is also worth emphasising that the results, as well as the resulting conclusions, may prove helpful in understanding the phenomena occurring, in particular, during working conditions under heavy load.

5. References

[1] Balta B., Sonmez F.O., Cengiz A.: Speed losses in V-ribbed belt drives. Mechanism and Ma-chine Theory. 2015, 86, 1–14, DOI: 10.1016/j.mechmachtheory.2014.11.016.

[2] Balta B., Sonmez F.O., Cengiz A.: Experimental identification of the torque losses in V-ribbed belt drives using the response surface method. Proceedings of the Institution of Mechanical Engineers. Part D: Journal of Automobile Engineering. 2015, 229(8), 1070–1082, DOI: 10.1177/0954407014555150.

[3] Belyaev A.K., Eliseev V.V., Irschik H., Oborin E.A.: Contact of two equal rigid pulleys with a belt modelled as Cosserat nonlinear elastic rod. Acta Mechanica. 2017, 228(12), 4425–4434, DOI: 10.1007/s00707-017-1942-0.

[4] Belyaev A.K., Eliseev V.V., Irschik H., Oborin E.A.: Dynamics of contour motion of belt drive by means of nonlinear rod approach. Dynamics and Control of Advanced Structures and Machines. 2019, 3, 21–29, DOI: 10.1007/978-3-319-90884-7_3.

[5] Bucchi F., Frendo F.: Analysis of belt transmissions capabilities using the brush model. Institute of Physics Conference Series: Materials Science and Engineering. 2021, 1038(1), DOI: 10.1088/1757-899X/1038/1/012076.

https://doi.org/10.14669/AM.VOL95.ART2

[6] Čepon G., Manin L., Boltežar M.: Experimental identification of the contact parameters between a V-ribbed belt and a pulley. Mechanism and Machine Theory. 2010, 45(10), 1424–1433, DOI: 10.1016/j.mechmachtheory.2010.05.006.

[7] Čepon G., Manin L., Boltežar M.: Introduction of damping into the flexible multibody belt-drive model: A numerical and experimental investigation. Journal of Sound and Vibration. 2009, 324(1–2), 283–296, DOI: 10.1016/j.jsv.2009.02.001.

[8] Čepon G., Manin L., Boltežar M.: Validation of a flexible multibody belt-drive model. Strojniški vestnik – Journal of Mechanical Engineering. 2011, 57(7–8), 539–546, DOI: 10.5545/sv-jme.2010.257.

[9] Chowdhury S., Yedavalli R.K.: Dynamics of belt-pulley-shaft systems. Mechanism and Machine Theory. 2016, 98, 199–215, DOI: 10.1016/j.mechmachtheory.2015.11.011.

[10] Cruz-Gómez M.A., Gallardo-Hernández E.A., Vite-Torrez M., Peña Bautista A.: Rubber steel friction in contaminated contacts. Wear. 2013, 302(1–2), 1421–1425, DOI: 10.1016/j.wear.2013.01.087.

[11] Dakel M., Jézéquel L., Sortais J.-L.: Stationary and transient analyses of a pulley-belt system based on an Eulerian approach. Mechanism and Machine Theory. 2018 128, 682–707, DOI: 10.1016/j.mechmachtheory.2018.07.002.

[12] Frendo F., Bucchi F.: "Brush model" for the analysis of flat belt transmissions in steady-state conditions. Mechanism and Machine Theory. 2020, 143, DOI: 10.1016/j.mechmachtheory.2019.103653.

[13] Higgins D.D., Marmo B.A., Jeffree C.E., Koutsos V., Blackford J.R.: Morphology of ice wear from rubber–ice friction tests and its dependence on temperature and sliding velocity. Wear. 2008, 265(5–6), 634–644, DOI: 10.1016/j.wear.2007.12.015.

[14] Hu Y., Zhu H., Zhu W.D., Li Ch., Pi Y.: Dynamic performance of a multi-ribbed belt based on an overlay constitutive model of carbon-black-filled rubber and experimental validation. Mechanical Systems and Signal Processing. 2017, 95, 252–272, DOI: 10.1016/j.ymssp.2017.03.013.

[15] Julio G., Plante J.S.: An experimentally-validated model of rubber-belt CVT mechanics. Mechanism and Machine Theory. 2011, 46(8), 1037–1053, DOI: 10.1016/j.mechmachtheory.2011.04.001.

[16] Kim D., Leamy M.J., Ferri A.A.: Dynamic Modeling and Stability Analysis of Flat Belt Drives Using an Elastic/Perfectly Plastic Friction Law. Journal of Dynamic Systems Measurement and Control – transactions of the ASME. 2011, 133(4), 1–10, DOI: 10.1115/1.4003796.

[17] Krawiec P., Waluś K., Warguła Ł., Adamiec J.: Wear evaluation of elements of V-belt transmission with the application of optical microscope. MATEC Web of Conferences. 2018, 157, 01009, DOI: 10.1051/matecconf/201815701009.

[18] Kubas K.: A model for the dynamic analysis of a belt transmission using the Dahl friction model. Journal of Theoretical and Applied Mechanics. 2017, 55(4), 1423–1435, DOI: 10.15632/jtam-pl.55.4.1423.

[19] Kubas K., Harlecki A.: Dynamic analysis of a belt transmission with the GMS friction model. Meccanica. 2021, 56(9), 2293–2305, DOI: 10.1007/s11012-021-01358-8.

[20] Leamy M.J., Wasfy T.M.: Analysis of belt-driven mechanics using a creep-rate-dependent friction law. ASME Journal of Applied Mechanics. 2002, 69(6), 763–771, DOI: 10.1115/1.1488663.

[21] Leamy M.J., Wasfy T.M.: Dynamic finite element modeling of belt drives. 18th Biennial Conference on Mechanical Vibration and Noise, ASME 2001 International Design Engineering Technical Conferences and Computers and Information in Engineering Conference. 2001, 6A, 365–371, DOI: 10.1115/DETC2001/VIB-21342.

[22] Leamy M.J., Wasfy T.M.: Transient and Steady-State Dynamic Finite Element Modeling of Belt-Drives. ASME Journal of Dynamic Systems, Measurement, and Control. 2002, 124(4), 575–581, DOI: 10.1115/1.1513793.

[23] Li K.W., Chen C.J.: The effect of shoe soling thread groove width on the coefficient of friction with different sole materials, floors, and contaminants. Applied Ergonomics. 2004, 35(6), 499–507, DOI: 10.1016/j.apergo.2004.06.010.

[24] Manin L., Liang X., Lorenzon C.: Power losses prediction in poly-v belt transmissions: application to front engine accessory drives. International Gear Conference. Lyon, Chandos Publishing. 2014, 1162–1171, DOI: 10.1533/9781782421955.1162.

[25] Manin L., Lorenzon C., Saad H.: Belt-pulley friction coefficient, experimental analysis: Influence of the Poly-V belt material components and contact pressure. Proceedings of the Inter-na-tional Conference on Power Transmissions. Chongqing, P.R. China, 2016, 0(191039), 47–51, DOI: 10.1201/9781315386829-9.

[26] Mascenik J., Murcinkowa Z.: Experimental determination of the belt transmission slip. Man-age-ment Systems in Production Engineering. 2019, 4(27), 205–210, DOI: 10.1515/mspe-2019-0032.

[27] Mofidi M., Kassfeldt E., Prakash B.: Tribological behaviour of an elastomer aged in different oils. Tribology International. 2008, 41(9–10), 860–866, DOI: 10.1016/j.triboint.2007.11.013.

[28] Oborin E., Vetyukov Y., Steinbrecher I.: Eulerian description of non-stationary motion of an idealized belt-pulley system with dry friction. International Journal of Solids and Structures. 2018, 147, 40–51, DOI: 10.1016/j.ijsolstr.2018.04.007.

[29] Oborin E.: Belt–pulley interaction: role of the action line of friction forces. Acta Mechanica. 2020, 231(9), 3979–3987, DOI: 10.1007/s00707-020-02724-5.

[30] Pan Y., Liu X., Shan Y., Chen G.(S.): Complex modal analysis of serpentine belt drives on beam coupling model. Mechanism and Machine Theory. 2017, 116, 162–177, DOI: 10.1016/j.mechmach-theory.2017.05.016.

[31] Silva C.A.F., Manin L., Andrianoely M.A., Besnier E., Redmond D.: Power losses distribution in serpentine belt drive: Modelling and experiments. Proceedings of the Institution of Mechanical Engineers. Part D. Journal of Automobile Engineering. 2019, 233(13), 3424–3437, DOI: 10.1177/0954407018824943.

[32] Yamaguchi T., Umetsu T., Ishizuka Y., Kasuga K., Ito T., Ishizawa S., et al.: Development of new foot-wear sole surface pattern for prevention of slip-related falls. Safety Science. 2012, 50(4), 986–994, DOI: 10.1016/j.ssci.2011.12.017.